Magnetic and crystal structures of $Er_5(Si_xGe_{1-x})_4$

2006 J. Phys.: Condens. Matter 18 3937

(http://iopscience.iop.org/0953-8984/18/16/004)

INSTITUTE OF PHYSICS PUBLISHING JOURNAL OF PHYSICS: CONDENSED MATTER

J. Phys.: Condens. Matter **18** (2006) 3937–3950 doi:10.1088/0953-8984/18/16/004

Magnetic and crystal structures of $Er_5(Si_xGe_{1-x})_4$

C Ritter[1], C Magen[2], L Morellon[2,3,6], P A Algarabel[2], M R Ibarra[2,3], V K Pecharsky[4,5], A O Tsokol[4] and K A Gschneidner Jr[4,5]

[1] Institut Laue-Langevin, Boîte Postale 156, 38042 Grenoble Cédex 9, France
[2] Instituto de Ciencia de Materiales de Aragón, Universidad de Zaragoza and Consejo Superior de Investigaciones Científicas, 50009 Zaragoza, Spain
[3] Instituto de Nanociencia de Aragón, Universidad de Zaragoza, 50009 Zaragoza, Spain
[4] Ames Laboratory, Iowa State University, Ames, IA 50011-3020, USA
[5] Department of Materials Science and Engineering, Iowa State University, Ames, IA 50011-2300, USA

E-mail: morellon@unizar.es

Received 6 February 2006, in final form 28 February 2006
Published 3 April 2006
Online at stacks.iop.org/JPhysCM/18/3937

Abstract

The magnetic and crystallographic structures in the $Er_5(Si_xGe_{1-x})_4$ system have been investigated for $x = 1, 0.875$ and 0 using macroscopic magnetic measurements and neutron powder diffraction. The existence of a first-order structural transformation from a high-temperature orthorhombic O(I) structure to a low-temperature monoclinic M polymorph in the temperature range 160–220 K has been confirmed for Er_5Si_4. In contrast, compounds with $x = 0.875$ and 0 retain their room-temperature crystallographic phases—M and O(II), respectively—on cooling down to 2 K. Both Si-containing alloys adopt canted ferromagnetic structures below $T_C \cong 30$ K with an easy magnetization direction along the *b*-axis and a weak antiferromagnetic coupling in the (010) plane. The Er_5Ge_4 compound orders antiferromagnetically at $T_N = 14$ K in a complex incommensurate structure.

(Some figures in this article are in colour only in the electronic version)

1. Introduction

The family of intermetallic compounds—$R_5(Si_xGe_{1-x})_4$—where R is a rare earth metal, is characterized by a strong coupling of magnetic and crystallographic sublattices, which results in an intriguing interplay between several closely related layered crystal structures, each exhibiting a peculiar magnetic behaviour [1–3]. Associated with the ability of the magnetic field to induce magnetostructural transitions in many representatives of the family, a giant magnetocaloric effect [4, 5], giant magnetoresistance [6–8], and remarkably strong

[6] Author to whom any correspondence should be addressed.

magnetoelastic anomalies [9–11] have been discovered in compounds with R = Gd, which to date remains the most studied member of the family.

The first exception to the general behaviour of the Gd-based system was recently found in $Tb_5Si_2Ge_2$. Even though preliminary studies suggested that it behaves consistently with the phenomenology of the R = Gd alloys [12], a more thorough investigation of the presumed magnetostructural transformation in the $Tb_5Si_2Ge_2$ compound revealed that magnetic and crystallographic transformations here are not fully coupled. At room temperature, this alloy exists in the paramagnetic state adopting the monoclinic (space group $P112_1/a$) $Gd_5Si_2Ge_2$-type structure (M) that orders ferromagnetically (FM) at $T_C = 110$ K and subsequently transforms into an orthorhombic (space group *Pnma*) Gd_5Si_4-type state [O(I)] at $T_t = 100$ K [13]. An even more spectacular decoupling of the magnetic and structural transitions was reported in the Er_5Si_4 system [14]. This alloy had been commonly considered a simple ferromagnet ($T_C = 30$ K) exhibiting a room-temperature O(I) structure [15, 16]. However, a study of temperature dependence of its crystal structure has revealed a reversible crystallographic transformation on cooling to a low-temperature M phase in the temperature range between 200 and 230 K [14, 17]. In addition to the extended temperature span between the magnetic ($T_C = 30$ K) and crystallographic ($T_t = 200$–230 K) changes, the order of the crystallographic phases is opposite to that conventionally observed below room temperature in other $R_5(Si_xGe_{1-x})_4$ compounds, where the room temperature paramagnetic M phase always transforms into the O(I) modification on cooling, either simultaneously with the ferromagnetic ordering (e.g., $Gd_5Si_2Ge_2$), or first ordering ferromagnetically and then adopting the O(I) structure (e.g., $Tb_5Si_2Ge_2$).

This unusual change in the behaviour within the family as the R-component changes from Gd to Tb and then to Er calls for a more detailed examination of various compositions in the $Er_5(Si_xGe_{1-x})_4$ series in order to further probe microscopic features of possible structural and/or magnetostructural anomalies and the nature of the low-temperature magnetic state(s). With this aim, we have performed a complete macroscopic magnetic characterization and microscopic neutron scattering investigation of three selected members of the $Er_5(Si_xGe_{1-x})_4$ family corresponding to three different room-temperature crystallographic structures found to exist in these compounds [18].

2. Experimental details

Polycrystalline specimens of Er_5Si_4, $Er_5(Si_{0.875}Ge_{0.125})_4$ and Er_5Ge_4 have been synthesized by arc-melting of stoichiometric mixtures of high-purity (99.96 wt%) Er prepared by the Materials Preparation Center of the Ames Laboratory [19], and high-purity (99.9999 wt%) Si and Ge that were purchased from a commercial vendor. Further details on the sample preparation can be found elsewhere [14, 17, 18]. The room-temperature x-ray diffraction patterns collected from the three specimens studied in the present work have confirmed that Er_5Si_4 crystallizes in the orthorhombic *Pnma* Gd_5Si_5-type O(I) structure. The addition of a small amount of Ge brings about a change of crystal symmetry, and the $Er_5(Si_{0.875}Ge_{0.125})_4$ alloy exhibits at room temperature the monoclinic $P112_1/a$ $Gd_5Si_2Ge_2$-type M phase. Finally, the second terminal compound in this pseudobinary system—Er_5Ge_4—adopts the orthorhombic *Pnma* symmetry, but with a different atomic arrangement that is typical of the Gd_5Ge_4-type O(II) structure.

Magnetization experiments have been performed in a commercial (Quantum Design) superconducting quantum interference device (SQUID) magnetometer in the temperature range 5–300 K and in magnetic fields up to 50 kOe. Neutron diffraction experiments have been carried out using the high-resolution powder diffractometer D2B ($\lambda = 1.596$ Å) and the high-intensity powder diffractometer D1B ($\lambda = 2.52$ Å), both at the Institute Laue–Langevin (ILL)

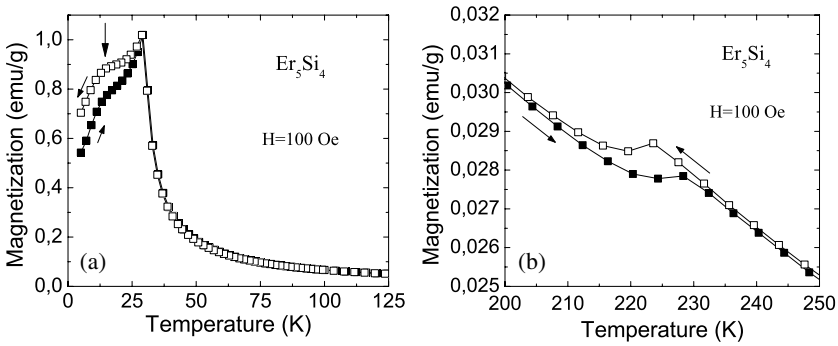

Figure 1. The temperature dependence of the magnetization of Er_5Si_4 measured in a 100 Oe magnetic field on heating of a zero-field-cooled sample (solid squares) and cooling (open squares). (a) The low-temperature magnetic transition. (b) The high-temperature anomaly associated with the O(I) $\leftrightarrow$ M structural transformation.

in Grenoble, France. The complete neutron diffraction patterns have been collected at selected temperatures between $2\theta = 5°$ and 165° in D2B. Temperature scans have been measured in D1B in the temperature range 2–300 K. Crystallographic and magnetic structures have been refined by analysing the neutron diffraction patterns collected in D2B with the Rietveld method using the software package FULLPROF [20].

3. Macroscopic magnetic characterization

The bulk magnetic characterization of the three alloys has been performed in order to refine their macroscopic magnetic behaviour and check reproducibility of the results previously reported [18] for the nominal compositions Er_5Si_4, $Er_5(Si_{0.875}Ge_{0.125})_4$, and Er_5Ge_4. Figure 1(a) displays the magnetization of Er_5Si_4 at low temperature in a magnetic field of 100 Oe, where a sharp peak is observed at $T_C = 30$ K. A secondary shoulder (marked with a vertical arrow) is found at $T' \cong 17$ K, which was previously associated with an ErSi impurity phase present in this compound and that has a T_C of 11.5 K [14]. Recently, a spin reorientation process has also been reported in an orthorhombic Er_5Si_4 specimen[7] between 4 and 14 K [21], and a similar magnetic behaviour is rather plausible in our monoclinic Er_5Si_4 phase.

The high-temperature paramagnetic state presents distinct steps in magnetization as seen in figure 1(b) in both the heating and cooling curves associated with the O(I) $\leftrightarrow$ M crystallographic transformation. The change of the crystal structure and the hysteretic behaviour give rise to a small loop in the magnetization at $T \cong 210$–230 K. No perceptible change in the effective magnetic moment is induced by the structural transformation within the experimental accuracy, being $\mu_{eff} = 9.1(1)\ \mu_B$ for the high-temperature O(I) phase and $\mu_{eff} = 9.0(1)\ \mu_B$ in the low-temperature M state. These values are somewhat smaller as compared either with those reported earlier [18] or with the theoretical paramagnetic moment of free Er^{3+}

[7] A sample of Er_5Si_4 studied in [21] retains orthorhombic O(I) structure down to 3.6 K. The difference between this sample and the one studied here is that the former was prepared from a commercial-grade, '99.9% pure' Er metal, as were the other Er_5Si_4 samples studied earlier [15, 16]. These samples apparently do not exhibit an O(I) $\rightarrow$ M transition on cooling below room temperature. It is, therefore, reasonable to assume that interstitial impurities (such as C, O and F, which are found in concentrations ranging from $\sim 10^3$ to $\sim 10^4$ parts per million atomic in most commercial '99.9%' pure rare earth metals, and whose concentrations in the rare earth metals prepared by the Materials Preparation Center of the Ames Laboratory [19] are usually on the order of 10^2 ppma [22]), are responsible for destroying the structural-only transformation in Er_5Si_4 around 200–230 K.

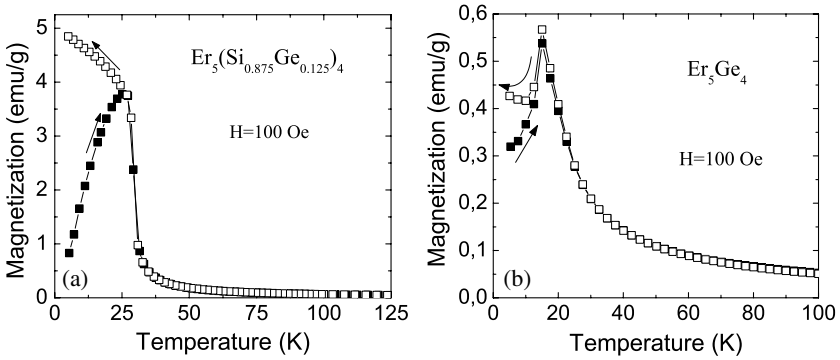

Figure 2. The temperature dependences of the magnetization of (a) $Er_5(Si_{0.875}Ge_{0.125})_4$ and (b) Er_5Ge_4 measured in a 100 Oe magnetic field during heating of zero-field-cooled samples (solid squares) and cooling (open squares).

ion of 9.58 μ_B. The most likely reason is that moments here have been determined from low-field data, and the values may be easily affected by a small amount of a ferromagnetic impurity undetected by any other techniques, and/or may be intrinsic, since all R_5T_4 compounds show deviations from Curie–Weiss behaviour in low fields due to high-temperature spin fluctuations, short-range correlations [23] or even the presence of ferromagnetic clusters [24]. The change in the strength of the magnetic correlations due to the making (high temperature O(I) phase) or breaking (low temperature M phase) of covalent-like Si–Si bonds is evidenced by a marked change in the paramagnetic Weiss temperature, i.e. $\Theta_P \cong 34$ K and $\Theta_P \cong 18$ K for the high-temperature O(I) state and low-temperature M phase, respectively. The higher Weiss temperature of the orthorhombic phase reflects the influence of the O(I) structure that favours the FM interactions due to the formation of a three-dimensional network of the interlayer –Er–Si–Si–Er– bonds promoting superexchange interactions in addition to a conventional RKKY indirect exchange mediated by conduction electrons [1, 25].

In the case of $Er_5(Si_{0.875}Ge_{0.125})_4$, a similar set of measurements has been carried out, and the experimental results are displayed in figure 2(a). A ferromagnetic-like ordering is seen at low temperature with a Curie temperature $T_C = 29$ K, determined as the maximum of the derivative $|(dM/dT)_H|$. In this case, no anomalies are observed below T_C, but a notable difference in the magnitude of the magnetic signal is observed when compared with Er_5Si_4. As we will show later, the approximately fivefold increase of the magnetization is not due to the intrinsic change of the magnetic properties at the $x = 0.875$ stoichiometry, but it may be related to a preferred orientation of the grains of the polycrystalline specimen combined with a significant magnetocrystalline anisotropy as evidenced by a large difference between the zero-field-cooling measurement on heating and the field-cooling experiment. In the paramagnetic state, a typical Curie–Weiss behaviour is observed with $\Theta_P \cong 22$ K and $\mu_{eff} = 8.85(1)\ \mu_B$. The reasons for this smaller-than-expected value are as mentioned before in the case of Er_5Si_4. No anomaly similar to the high-temperature transition in Er_5Si_4 is observed in the whole temperature range, which indicates that no structural change takes place in this alloy when cooling through the paramagnetic regime.

As follows from an early characterization performed by Holtzberg *et al* [15] and a recent one by Pecharsky *et al* [18], the germanide Er_5Ge_4 is expected to be antiferromagnetic (AFM). Our magnetization data plotted in figure 2(b) display a peak-like anomaly at $T_N = 15$ K. No slope changes are found in the whole temperature range, and a small zero-field-cooled heating/field-cooling difference seen in figure 2(a) is also likely due to magnetocrystalline

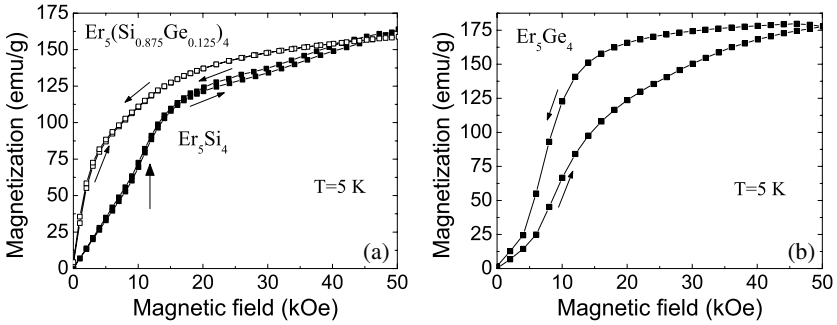

Figure 3. Low-temperature magnetization isotherms of the zero-field-cooled $Er_5(Si_xGe_{1-x})_4$ compounds measured at 5 K: (a) Er_5Si_4 and $Er_5(Si_{0.875}Ge_{0.125})_4$, and (b) Er_5Ge_4.

anisotropy. The fit of the high-temperature inverse paramagnetic susceptibility to a Curie–Weiss model results in $\Theta_P \cong 3$ K and $\mu_{eff} \cong 9.6\ \mu_B$. Low but positive value of the paramagnetic Weiss temperature may be reflective of the existence of weak FM interactions in Er_5Ge_4.

It is interesting to compare the low-temperature magnetization as a function of the magnetic field of three different compounds. In figure 3(a), we show the magnetization isotherms of Er_5Si_4 and $Er_5(Si_{0.875}Ge_{0.125})_4$, whereas isothermal magnetization behaviour of Er_5Ge_4 is depicted in 3(b). From the saturation magnetization, it is evident in all cases that the $Er_5(Si_xGe_{1-x})_4$ system is not a simple ferromagnet at low temperatures. The magnetization at 50 kOe is always far from the theoretical saturation value of 9 μ_B/Er, i.e. it reaches 5.6, 5.4 and 7.2 μ_B/Er for $x = 1$, 0.875 and 0, respectively. This fact, in addition to the shapes of the isotherms, reflects the existence of clearly non-collinear magnetic structures, e.g. a strongly canted ferromagnet or a ferrimagnet. In the case of Er_5Si_4, a metamagnetic process (marked with a vertical arrow) takes place in magnetic fields between 10 and 15 kOe. This is followed by a hysteretic regime above 20 kOe. It appears that the magnetic field is capable of transforming the zero-field M crystallographic phase into a high-field O(I) state by enhancing FM interactions that result in a formation of a nearly collinear ferromagnetic structure [26].

In the case of Er_5Ge_4, a more dramatic metamagnetic behaviour is followed by an extended hysteresis existing over the whole range of fields, which suggests that magnetic fields lower than 10 kOe are capable of inducing remarkable changes in the magnetism of Er_5Ge_4 related to a metamagnetic field-induced AFM $\rightarrow$ FM transformation. In both cases (Er_5Si_4 and Er_5Ge_4), the initial magnetic state seems to be recovered when magnetic field is reduced to zero. The Si-rich $Er_5(Si_{0.875}Ge_{0.125})_4$ shows a ferromagnetic-like increase of the magnetization in low fields, yet again saturation magnetization is too small when compared with the expected value.

4. Neutron diffraction results

4.1. Er_5Si_4

Neutron diffraction thermal scans of Er_5Si_4 have been collected on D1B in the temperature range 2–250 K and they are illustrated in figure 4, where details of the mid-angle and low-angle spectra are depicted. These experiments confirm the existence of an O(I) $\rightarrow$ M structural transformation that begins on cooling around 210 K, as can be seen in figure 4(a). For the low-temperature magnetic ordering, this transition is clearly observed in the neutron diffraction spectra by the development of low-angle magnetic reflections seen in figure 4(b). The onset of

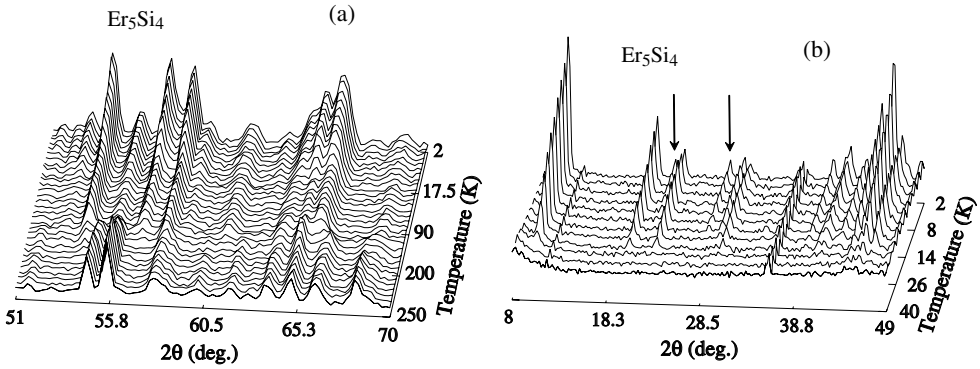

Figure 4. Details of the neutron D1B thermodiffractogram of Er_5Si_4: (a) the high-temperature O(I) $\leftrightarrow$ M structural phase transformation and (b) the low-temperature magnetic ordering transition (note the non-linear scales of temperature). Selected peaks revealing the spin reorientation transition at $T \sim 15$ K are marked with arrows.

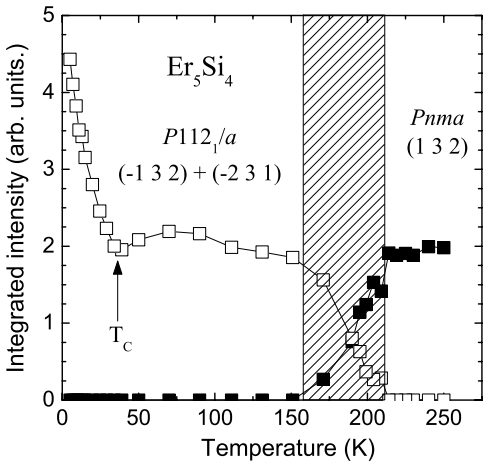

Figure 5. Integrated intensities of selected Bragg peaks associated with the crystallographic phases involved in the structural transformation of Er_5Si_4 (measured on cooling). The filled squares represent the intensity of one of the O(I) peaks indexed as (132), whereas empty squares represent the combined intensity of $(\bar{1}32)$ and $(\bar{2}31)$ peaks of the M phase. The dashed area depicts the phase coexistence region.

the magnetic state occurs around $T_C = 30$ K, and a second process is observed around $\sim$15 K, suggesting the existence of a spin reorientation transition. An increase of the intensity of many nuclear (Bragg) peaks is evident due to the superimposed magnetic scattering, but none of the Bragg peaks disappears, thus indicating that no structural change accompanies the magnetic ordering at low temperature. A large number of new reflections at low angles that are absent in the high-temperature regime develop below the transition temperature. This indicates the existence of a significant AFM component in the magnetic structure of the erbium silicide. In order to further illustrate the evolution of different phases involved, figure 5 depicts integrated intensities of two Bragg peaks: the orthorhombic (132) and the nearly overlapped monoclinic $(\bar{1}32)$ and $(\bar{2}31)$ showing that M and O(I) phases of Er_5Si_4 coexist in the temperature range 160–210 K, as highlighted by the dashed region. Phase coexistence clearly underlines the

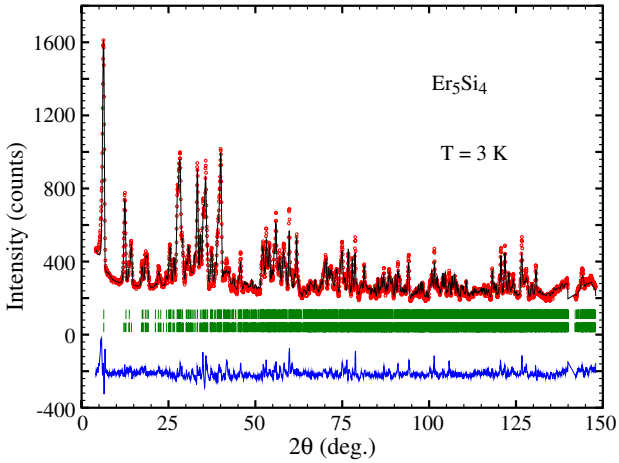

Figure 6. Neutron powder diffraction pattern of Er_5Si_4 compound collected at $T = 3$ K in the high-resolution D2B diffractometer. The experimental data (dots), the theoretical curve (line drawn through the data points) and the difference between them (line at the bottom of the plot) are shown. The vertical bars indicate the calculated positions of crystallographic (top) and magnetic (bottom) reflections allowed by the corresponding crystallographic and magnetic space groups.

thermo-elastic character of the structural transformation. A sharp increase of the intensity of the two overlapped Bragg peaks of the M phase also indicates that monoclinic Er_5Si_4 develops an FM ordering component below 30 K.

The structural and magnetic parameters of Er_5Si_4 phases have been refined using neutron diffraction patterns collected in the high-resolution D2B diffractometer at $T = 295$, 40, 20 and 3 K. As an example, we present the data collected at the lowest temperature (3 K) in figure 6. The crystallographic parameters resulting from the refinements are summarized in table 1, and the magnetic moments of Er atoms determined from the low-temperature fits are listed in table 2. The room-temperature refinement at 295 K confirms that this Er_5Si_4 specimen crystallizes in the *Pnma* space group adopting the Gd_5Si_4-type O(I) crystallographic phase. At 40 K, the compound is in a low-temperature polymorphic modification exhibiting monoclinic space group symmetry $P112_1/a$ and the $Gd_5Si_2Ge_2$-type M crystallographic phase. The lattice parameters are in good agreement with previous reports on Er_5Si_4 taking into account the difference in data collection temperatures and also in the techniques (single-crystal and powder x-ray diffraction in references [14, 16, 17] versus powder neutron diffraction in this work). A large volume change is indeed observed during the high-temperature transition, even though there is almost no difference between the unit-cell volumes listed in table 1 for 295 and 40 K. This is because the volume discontinuity obtained from the refinements at these temperatures should be corrected by a typical thermal expansion for this family of compounds from 295 to 40 K of $\Delta V/V \cong 2.5 \times 10^{-5}$ K^{-1} [27]. A more realistic volume discontinuity then becomes $\Delta V/V \cong +0.7\%$ on cooling through the transition, and the expected anisotropic changes of the lattice parameters at the transition temperature are $\Delta a/a \cong +1.1\%$, $\Delta b/b \cong +0.16\%$ and $\Delta c/c \cong -0.4\%$.

The magnetic structure of Er_5Si_4 at low temperature has been refined assuming its commensurability with the crystal structure, i.e. by testing magnetic space groups associated with the crystallographic space group $P112_1/a$ for a propagation vector $\boldsymbol{\tau} = (000)$ extracted from [28] and detailed in table 3. The best convergence has been obtained using the magnetic space group $P112_1'/a$ with the spins in the 4e sites ordered following magnetic modes $F_xF_yG_z$.

Table 1. Crystallographic parameters of Er_5Si_4 refined from D2B neutron diffraction data collected at $T = 295$, 40, 20 and 3 K.

Temperature		295 K			40 K	20 K	3 K
Space group		$Pnma$			$P112_1/a$	$P112_1/a$	$P112_1/a$
a (Å)		7.2896(3)			7.3519(2)	7.3528(2)	7.3525(3)
b (Å)		14.3667(6)			14.3590(5)	14.3567(5)	14.3566(7)
c (Å)		7.5947(3)			7.5478(2)	7.5466(2)	7.5453(3)
γ (deg.)		90			93.201(3)	93.201(3)	93.233()
V (Å^3)		795.37(6)			795.58(4)	795.40(4)	795.18(6)
Er1 (4c) :	x	0.344(1)	Er1 (4e):	x	0.324(1)	0.325(1)	0.326(1)
	y	1/4		y	0.2461(5)	0.2454(5)	0.2454(6)
	z	0.990(9)		z	0.0022(9)	0.0045(8)	0.005(1)
Er2 (4c) :	x	0.0169(7)	Er2A (4e):	x	−0.0062(9)	−0.0045(9)	−0.0060(9)
	y	0.0962(3)		y	0.0965(5)	0.0973(5)	0.0971(6)
	z	0.8177(7)		z	0.1812(9)	0.181(1)	0.179(1)
			Er2B (4e):	x	0.0094(9)	0.0138(7)	0.0151(8)
				y	0.4014(5)	0.4008(4)	0.4004(6)
				z	0.183(1)	0.1809(8)	0.179(1)
Er3 (8d) :	x	0.1776(7)	Er3A (4e):	x	0.3561(9)	0.3555(8)	0.356(1)
	y	0.1232(3)		y	0.8812(4)	0.8805(5)	0.8797(6)
	z	0.32009		z	0.1696(9)	0.168(1)	0.172(1)
			Er3B (4e):	x	0.3348(8)	0.3316(8)	0.331(1)
				y	0.6238(4)	0.6235(4)	0.6218(5)
				z	0.178(1)	0.1796(9)	0.179(1)
Si1 (4c) :	x	0.966(2)	Si1 (4e):	x	0.954(2)	0.948(2)	0.947(4)
	y	1/4		y	0.254(9)	0.254(1)	0.259(2)
	z	0.115(1)		z	0.893(2)	0.894(2)	0.889(3)
Si2 (4c) :	x	0.207(1)	Si2 (4e):	x	0.216(2)	0.213(2)	0.214(3)
	y	1/4		y	0.2524(8)	0.253(1)	0.254(2)
	z	0.366(1)		z	0.367(2)	0.361(2)	0.361(3)
Si3 (8d) :	x	0.164(2)	Si3A (4e):	x	0.203(2)	0.200(2)	0.199(4)
	y	0.9608(6)		y	0.9626(9)	0.962(1)	0.963(2)
	z	0.529(1)		z	0.465(2)	0.469(2)	0.475(4)
			Si3B (4e):	x	0.150(2)	0.150(3)	0.145(4)
				y	0.5403(8)	0.540(1)	0.539(2)
				z	0.477(2)	0.476(2)	0.481(4)
R_p/R_{wp} (%)		3.3/4.7			2.7/3.6	3.2/4.2	4.8/6.4
R_{Bragg} (%)		18.3[a]			13.2	11.4	12.3
R_{mag} (%)						10.4	10.7
χ^2		6.2			6.0	5.4	11.9

[a] This relatively larger value is likely related to some unaccounted small fraction of the monoclinic polymorph [18] or to the presence of internal strain, stacking faults, or preferred orientation.

As can be seen in figure 7(a), the spin arrangement at 20 K corresponds to a complex non-collinear ferromagnet with an easy magnetization direction along the b-axis in a zero magnetic field. A weak AFM coupling is observed in the (010) plane; Er moments forming small canting angles with the b-direction $\theta_{Er1} \cong 9°$, $\theta_{Er2A} \cong 10°$, $\theta_{Er2B} \cong 25°$, $\theta_{Er3A} \cong 7°$, and $\theta_{Er3B} \cong 43°$.

Magnetic moments of the Er atoms nearest to the silicon atoms that form interlayer Si–Si covalent-like bonds (Er2B and Er3B positions) are greater than moments of those Er atoms that

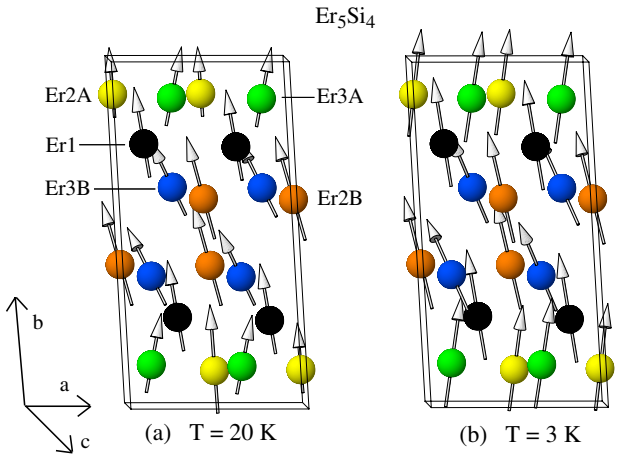

Figure 7. Arrangement of spins in the monoclinic Er_5Si_4 at $T = 20$ K (a) and $T = 3$ K (b).

Table 2. Components of the magnetic moments of Er atoms in Er_5Si_4 at $T = 20$ and 3 K.

Atoms	μ_x (μ_B)		μ_y (μ_B)		μ_z (μ_B)		μ_{total} (μ_B)	
(4e site)	20 K	3 K	20 K	3 K	20 K	3 K	20 K	3 K
Er1	−1.2(3)	−1.7(3)	5.0(2)	7.6(2)	−0.8(2)	−1.5(2)	5.3(1)	8.0(2)
Er2A	−0.1(2)	2.3(2)	2.2(2)	6.9(2)	−0.4(1)	−2.6(1)	2.3(1)	7.6(2)
Er2B	−2.8(2)	−2.7(2)	6.4(2)	7.5(2)	−3.0(2)	−3.5(1)	7.7(2)	8.8(2)
Er3A	1.6(2)	3.0(2)	3.4(1)	7.6(2)	0.4(2)	1.9(2)	3.7(2)	8.2(2)
Er3B	−2.7(2)	−3.6(3)	3.3(2)	4.7(2)	3.0(2)	5.8(2)	5.3(2)	8.5(2)

Table 3. Magnetic modes of the inequivalent positions with 4*e* site symmetry of the four possible magnetic space groups based on the crystallographic space group $P112_1/a$ associated with the magnetic propagation vector, $\boldsymbol{\tau} = (000)$.

				$P112_1/a$	$P112_1/a'$	$P112'_1/a$	$P112'_1/a'$
i	Position in the 4e site			$C_xC_yA_z$	$G_xG_yF_z$	$F_xF_yG_z$	$A_xA_yC_z$
1	x	y	z	+ + +	+ + +	+ + +	+ + +
2	(1/2)−x	−y	(1/2)+z	+ + −	− − +	+ + −	− − +
3	−x	−y	−z	− − −	+ + +	+ + +	− − −
4	(1/2)+x	y	(1/2)−z	− − +	− − +	+ + −	+ + −

are nearest to the broken Si–Si bonds (Er2A and Er3A). This is consistent with the magnetic structures of other monoclinic 5:4 phases, which indicates that the existence of covalent-like bonds reinforces the FM interactions, giving rise to higher net magnetic moments [13, 28]. Figure 7(b) illustrates the magnetic structure at the lowest temperature (3 K), i.e. below the second magnetic anomaly found around 15 K in D1B. The resulting magnetic state is similar to the 20 K magnetic structure with the following canting angles of the Er atoms: $\theta_{Er1} \cong 11°$, $\theta_{Er2A} \cong 21°$, $\theta_{Er2B} \cong 25°$, $\theta_{Er3A} \cong 14°$ and $\theta_{Er3B} \cong 51°$. The net magnetic moments rise in all of the Er sites, although the increase is greater in the 'ErA' positions.

It is noteworthy that the low-temperature M crystallographic structure of Er_5Si_4 does not agree with the O(I) low-temperature state reported by Cadogan *et al* [21]. As noted above, this is consistent with the use of commercial-purity Er loaded with interstitial impurities, which are known to hinder structural transformations in the 5:4 phases [29, 30]. Higher

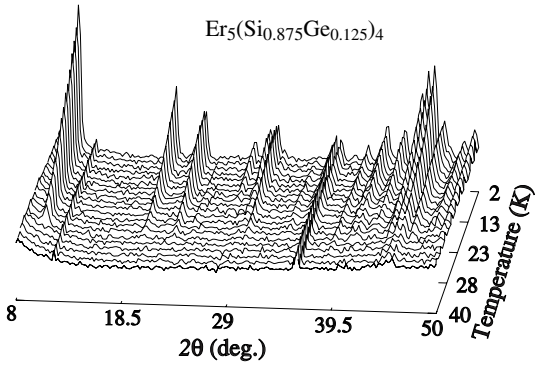

Figure 8. Details of the low-angle region of the D1B neutron thermodiffractogram of $Er_5(Si_{0.875}Ge_{0.125})_4$ (note the non-linear scale of temperatures).

purity of the Er metal, therefore, is an enabling factor promoting the occurrence of the high-temperature (around 200 K) structural transformation and the low-temperature M state. Overall, the magnetic structure of the monoclinic Er_5Si_4 is comparable with that reported in [21] (FM coupling along the *b*-axis with AFM components in the (010) plane), but the FM ordering in the orthorhombic Er_5Si_4 takes place at a slightly higher Curie temperature of 32(3) K. Even though it is difficult to derive definite conclusions because of different concentrations of impurities in two Er_5Si_4 samples, a small increase of the ordering temperature is consistent with the enhancement of FM interactions via the network of Si–Si covalent-like interlayer bonds in the O(I) structure described in [21].

4.2. $Er_5(Si_{0.875}Ge_{0.125})_4$

The D1B neutron thermodiffractogram of $Er_5(Si_{0.875}Ge_{0.125})_4$ shows no crystallographic transition on cooling down to the magnetic ordering temperature, and subsequently detailed experiments were performed only in the temperature range between 4 and 40 K; see figure 8. Below 40 K, the monoclinic $P112_1/a$ $Gd_5Si_2Ge_2$-type M phase is conserved down to the lowest temperature. As in Er_5Si_4, the magnetic ordering is signalled by the appearance of purely magnetic low-angle peaks around $T \cong 29.5$ K. Just as in Er_5Si_4, appearance of yet additional magnetic reflections at and below ∼10 K indicates a spin reorientation transition in $Er_5(Si_{0.875}Ge_{0.125})_4$.

The refinement of the crystal and magnetic structures has been carried out based on high-resolution D2B diffractograms taken at $T = 295$, 40, 20 and 2 K; the pattern collected at the lowest temperature ($T = 2$ K) is depicted in figure 9. The crystallographic parameters and the magnetic moment components that result from the fits are listed in tables 4 and 5, respectively. As in pure silicide, the magnetic space group resulting in the best refinements of the magnetic part of the spectra is $P112_1'/a$ with the magnetic modes $F_xF_yG_z$ in all cases. The magnetic structure below the ordering temperature is illustrated in figure 10(a) and it closely resembles that found in Er_5Si_4, i.e. there is a strong FM coupling along the *b*-direction with a small AFM canting along both the *a*- and *c*-axes. This confirms the extrinsic nature of the different magnetic behaviour observed in macroscopic measurements; see figure 2. The difference is in the values of the canting angles with respect to the *b*-axis, which in $Er_5(Si_{0.875}Ge_{0.125})_4$ are $\theta_{Er1} \cong 1°$, $\theta_{Er2A} \cong 10°$, $\theta_{Er2B} \cong 33°$, $\theta_{Er3A} \cong 5°$ and $\theta_{Er3B} \cong 43°$. Again, the Er2B and Er3B sites have larger magnetic moments compared to the Er2A and Er3A sites. The second

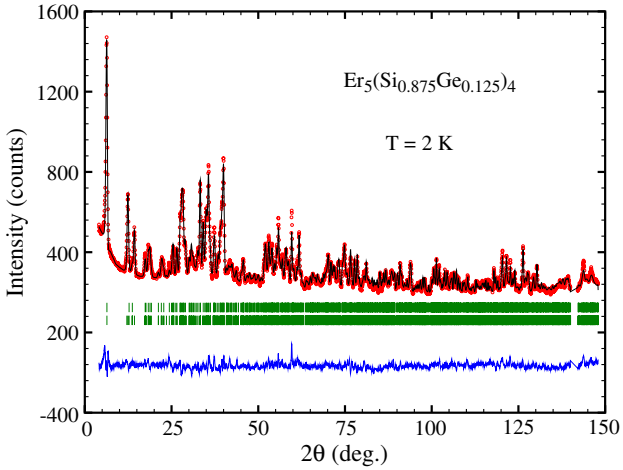

Figure 9. Neutron powder diffraction patterns of $Er_5(Si_{0.875}Ge_{0.125})_4$ alloy collected at $T = 2$ K in a D2B diffractometer. The experiment (dots), the calculated pattern (line drawn through the data points) and the difference between them (line at the bottom of the plot) are shown. The vertical bars indicate the calculated positions of Bragg (upper set) and magnetic (lower set) reflections.

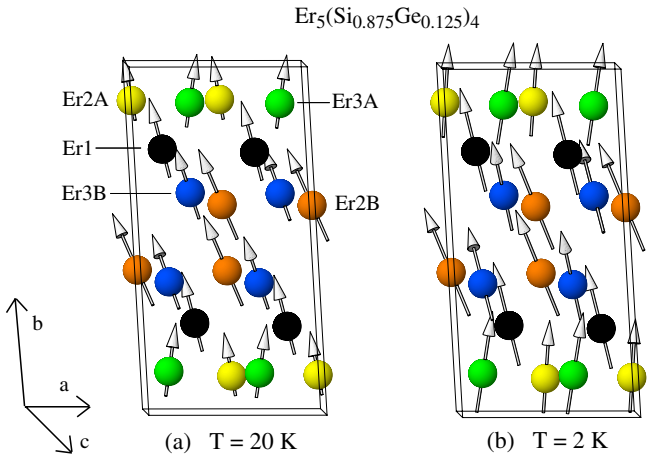

Figure 10. Magnetic structures of $Er_5(Si_{0.875}Ge_{0.125})_4$ at $T = 20$ K (a) and $T = 2$ K (b).

magnetic anomaly at 10 K gives rise to the magnetic structure plotted in figure 10(b), which is analogous to that of Er_5Si_4 at 3 K and the following are the canting angles with the b-axis: $\theta_{Er1} < 1°$, $\theta_{Er2A} \cong 39°$, $\theta_{Er2B} \cong 26°$, $\theta_{Er3A} \cong 50°$ and $\theta_{Er3B} \cong 32°$. The similarity of the magnetic structures of $Er_5(Si_xGe_{1-x})_4$ when $x = 1$ and 0.875 is consistent with the identical crystal structures and close stoichiometries.

4.3. Er_5Ge_4

Similar to the monoclinic $Er_5(Si_{0.875}Ge_{0.125})_4$, pure germanide Er_5Ge_4 exhibits no structural change on cooling from room temperature down to 2 K. The high-temperature orthorhombic O(II) phase is preserved at low temperatures, as can be seen in the D1B data presented in figure 11. The system orders magnetically at $T_N = 14$ K, which agrees well with the macroscopic magnetization measurements (see figure 2(b)). Below T_N, a second magnetic

Table 4. Crystallographic parameters of $Er_5(Si_{0.875}Ge_{0.125})_4$ refined from D2B data collected at $T = 295$, 40, 20 and 2 K. M is a statistical mixture of 87.5% Si and 12.5% Ge atoms, which was assumed to be unchanged from one site to another, and therefore not refined.

Temperature		295 K	40 K	20 K	2 K
Space group		$P112_1/a$	$P112_1/a$	$P112_1/a$	$P112_1/a$
a (Å)		7.3690(5)	7.3643(2)	7.3658(2)	7.3656(2)
b (Å)		14.404(1)	14.3713(5)	14.3700(4)	14.3683(6)
c (Å)		7.5712(6)	7.5579(2)	7.5568(2)	7.5558(2)
γ (deg)		92.944(6)	93.157(3)	93.216(2)	93.247(3)
V (Å^3)		802.5(1)	798.69(4)	798.61(4)	798.36(5)
Er1 (4e):	x	0.328(2)	0.325(1)	0.322(1)	0.325(1)
	y	0.2456(6)	0.2447(5)	0.2455(5)	0.2453(5)
	z	−0.002(1)	0.0017(9)	0.0031(8)	0.0024(8)
Er2A (4e):	x	−0.006(1)	−0.0082(9)	−0.0087(8)	−0.0086(8)
	y	0.0988(6)	0.0989(5)	0.0998(5)	0.0992(5)
	z	0.185(1)	0.1845(9)	0.182(1)	0.181(1)
Er2B (4e):	x	0.001(1)	0.004(1)	0.0096(8)	0.0104(8)
	y	0.4029(7)	0.4012(5)	0.4015(4)	0.4012(5)
	z	0.190(1)	0.1821(9)	0.1806(8)	0.1796(9)
Er3A (4e):	x	0.353(1)	0.3559(9)	0.3580(8)	0.3580(9)
	y	0.8813(6)	0.8806(4)	0.8824(4)	0.8815(5)
	z	0.159(1)	0.1634(9)	0.169(1)	0.172(1)
Er3B (4e):	x	0.328(1)	0.3342(9)	0.3313(8)	0.3316(8)
	y	0.6251(6)	0.6233(4)	0.6234(4)	0.6225(4)
	z	0.170(1)	0.1780(9)	0.1784(9)	0.178(1)
M1 (4e):	x	0.953(2)	0.943(2)	0.943(2)	0.938(3)
	y	0.252(1)	0.2507(8)	0.2538(9)	0.254(1)
	z	0.895(2)	0.891(1)	0.894(2)	0.904(2)
M2 (4e):	x	0.217(2)	0.212(1)	0.208(2)	0.212(2)
	y	0.248(1)	0.2500(8)	0.2503(8)	0.247(1)
	z	0.367(2)	0.367(2)	0.359(1)	0.356(2)
M3A (4e):	x	0.201(2)	0.204(2)	0.204(2)	0.209(3)
	y	0.965(1)	0.9601(8)	0.9628(8)	0.965(1)
	z	0.468(1)	0.464(2)	0.472(2)	0.471(3)
M3B (4e):	x	0.164(2)	0.159(2)	0.161(2)	0.158(3)
	y	0.537(1)	0.5388(7)	0.5390(8)	0.538(1)
	z	0.464(2)	0.468(1)	0.464(2)	0.467(2)
R_p/R_{wp} (%)		1.8/2.5	2.5/3.3	2.5/3.3	3.5/4.6
R_{Bragg} (%)		13.0	13.8	12.4	12.0
R_{mag} (%)				8.1	9.7
χ^2		6.1	3.5	6.2	8.5

anomaly occurs at $T' = 7$ K. Unfortunately, our study of Er_5Ge_4 is limited to the D1B thermodiffractograms, as it has not been possible to determine the magnetic state from the low-temperature D2B diffractogram due to the complexity of the magnetic peak structure. It appears that, unlike the other two members of the $Er_5(Si_xGe_{1-x})_4$ family, Er_5Ge_4 adopts an incommensurate magnetic structure, but we were unable to determine the presumably two- or three-non-zero-component propagation vector that describes the magnetic structure satisfactorily. Considering the complexity of the powder neutron diffraction data, a single

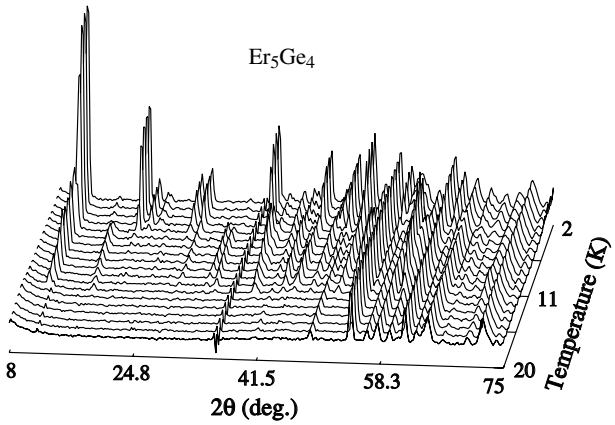

Figure 11. Low-temperature thermo-diffractogram of Er_5Ge_4 collected in D1B diffractometer.

Table 5. Components of magnetic moments of Er atoms in $Er_5(Si_{0.875}Ge_{0.125})_4$ at $T = 20$ and 3 K.

Atoms (4e site)	μ_x (μ_B)		μ_y (μ_B)		μ_z (μ_B)		μ_{total} (μ_B)	
	20 K	2 K	20 K	2 K	20 K	2 K	20 K	2 K
Er1	−1.4(3)	−2.5(2)	3.5(2)	6.6(2)	−0.1(1)	−0.0(1)	3.9(1)	7.2(2)
Er2A	−0.3(2)	1.3(2)	1.4(2)	5.3(2)	−0.3(1)	−1.3(1)	1.5(1)	5.5(2)
Er2B	−3.6(2)	−4.5(2)	4.8(2)	6.6(2)	−3.1(1)	−3.8(1)	6.8(1)	9.0(2)
Er3A	1.0(2)	2.6(2)	2.6(1)	6.3(1)	0.2(2)	1.5(1)	2.8(2)	6.8(1)
Er3B	−1.6(2)	−1.7(2)	2.9(2)	4.7(2)	2.7(1)	6.0(1)	4.3(1)	7.9(1)

crystal is required in order to obtain additional information and determine the propagation vector describing incommensurately modulated magnetic structure of Er_5Ge_4 and to complete a satisfactory refinement of its parameters.

5. Conclusions

Selected compositions in the $Er_5(Si_xGe_{1-x})_4$ system with $x = 1$, 0.875 and 0, exhibiting different crystallographic structures at room temperature, have been characterized by means of magnetization and neutron powder diffraction measurements. The compound Er_5Si_4 crystallizes in a room-temperature Gd_5Si_4 type (O(I) state with space group $Pnma$) and undergoes a reversible first-order crystallographic phase transition on cooling to a $Gd_5Si_2Ge_2$ type (M state, space group $P112_1/a$) in the temperature range 160–220 K. The $Er_5(Si_{0.875}Ge_{0.125})_4$ alloy crystallizes in the M phase in the whole temperature range of 2–300 K, whereas the room-temperature structure of the pure germanide Er_5Ge_4 is Gd_5Ge_4-type (O(II) phase, space group $Pnma$) and it also shows no structural anomalies on cooling down to 2 K. For the compositions with $x = 1$ and 0.875, the magnetic structures have been refined in the magnetic space group $P112'_1/a$. Both are canted ferromagnetic structures with an easy magnetization axis along the b-axis exhibiting a weak antiferromagnetic canting in the (010) plane. In the case of Er_5Si_4, the magnetic structure is similar to that observed earlier in a specimen that preserves the O(I) structure over the entire range of temperatures. The Er_5Ge_4 alloy apparently adopts a complex incommensurate magnetic structure that has not been determined. It may have a two- or three-component propagation vector, and single-crystal neutron diffraction data are needed to fully characterize the microscopic magnetism of the

germanide. Although further investigation is required, macroscopic magnetic measurements indicate that a rather weak magnetic field ($H \leqslant 10$ kOe) induces a remarkable change of the magnetic properties of Er_5Ge_4.

Acknowledgments

The financial support of the Spanish MEC (MAT2005-05565-CO2) and Spanish DGA (grant no E26 and project PIP017/2005) is acknowledged by the University of Zaragoza. Work at the Ames Laboratory is supported by the Office of Basic Energy Sciences, Materials Sciences Division of the US Department of Energy under contract no W-7405-ENG-82 with Iowa State University.

References

[1] Pecharsky V K and Gschneidner K A Jr 2001 *Adv. Mater.* **13** 683
[2] Choe W, Pecharsky V K, Pecharsky A O, Gschneidner K A Jr, Young V G Jr and Miller G J 2000 *Phys. Rev. Lett.* **84** 4617
[3] Pecharsky V K and Gschneidner K A Jr 1997 *J. Alloys Compounds* **260** 98
[4] Pecharsky V K and Gschneidner K A Jr 1997 *Phys. Rev. Lett.* **78** 4494
[5] Pecharsky V K and Gschneidner K A Jr 1997 *Appl. Phys. Lett.* **70** 3299
[6] Morellon L, Stankiewicz J, García-Landa B, Algarabel P A and Ibarra M R 1998 *Appl. Phys. Lett.* **73** 3462
[7] Morellon L, Algarabel P A, Magen C and Ibarra M R 2001 *J. Magn. Magn. Mater.* **237** 119
[8] Levin E M, Pecharsky V K and Gschneidner K A Jr 1999 *Phys. Rev.* B **60** 7993
[9] Morellon L, Algarabel P A, Ibarra M R, Blasco J, García-Landa B, Arnold Z and Albertini F 1998 *Phys. Rev.* B **58** R14721
[10] Morellon L, Blasco J, Algarabel P A and Ibarra M R 2000 *Phys. Rev.* B **62** 1022
[11] Magen C, Morellon L, Algarabel P A, Marquina C and Ibarra M R 2003 *J. Phys.: Condens. Matter* **15** 2389
[12] Ritter C, Morellon L, Algarabel P A, Magen C and Ibarra M R 2002 *Phys. Rev.* B **65** 094405
[13] Morellon L, Ritter C, Magen C, Algarabel P A and Ibarra M R 2003 *Phys. Rev.* B **68** 024417
[14] Pecharsky V K, Pecharsky A O, Mozharivskyj Y, Gschneidner K A Jr and Miller G J 2003 *Phys. Rev. Lett.* **91** 207205
[15] Smith G S, Tharp A G and Johnson Q 1967 *Acta Crystallogr.* **22** 940
[16] Holtzberg F, Gambino R J and McGuire T R 1967 *J. Phys. Chem. Solids* **28** 2283
[17] Mozharivskyj Y, Pecharsky A O, Pecharsky V K, Miller G J and Gschneidner K A Jr 2004 *Phys. Rev.* B **69** 144102
[18] Pecharsky A O, Gschneidner K A Jr, Pecharsky V K, Schlagel D L and Lograsso T A 2004 *Phys. Rev.* B **70** 144419
[19] Materials Preparation Center, Ames Laboratory US-DOE, Ames, IA, USA (www.mpc.ameslab.gov)
[20] Rodriguez-Carvajal J 1993 *Physica* B **192** 55
Rodriguez-Carvajal J L and Roisnel T , http://www-llb.cea.fr/fullweb/fp2k/fp2k.htm
[21] Cadogan J M, Ryan D H, Altounian Z, Liu X and Swainson I P 2004 *J. Appl. Phys.* **95** 7076
[22] Gschneidner K A Jr 1993 *J. Alloys Compounds* **193** 1
[23] Casanova F, de Brion S, Labarta A and Batlle X 2005 *J. Phys. D: Appl. Phys.* **38** 3343
[24] Magen C, Algarabel P A, Morellon L, Araujo J P, Ritter C, Ibarra M R and Sousa J B, unpublished
[25] Levin E M, Pecharsky V K and Gschneidner K A Jr 2000 *Phys. Rev.* B **62** R14625
[26] Magen C, Ritter C, Morellon L, Algarabel P A, Ibarra M R, Tsokol A O, Pecharsky V K and Gschneidner K A Jr, unpublished
[27] Mudryk Ya, Holm A P, Gschneidner K A Jr and Pecharsky V K 2005 *Phys. Rev.* B **72** 064442
[28] Magen C, Ritter C, Morellon L, Algarabel P A and Ibarra M R 2004 *J. Phys.: Condens. Matter* **16** 7427
[29] Mozharivskyj Y, Pecharsky A O, Pecharsky V K and Miller G J 2005 *J. Am. Chem. Soc.* **127** 317
[30] Magen C, Morellon L, Algarabel P A, Ibarra M R, Ritter C, Pecharsky A O, Pecharsky V K and Gschneidner K A Jr 2004 *Phys. Rev.* B **70** 224429